Agronomy Research **15**(4), 1659–1673, 2017
https://doi.org/10.15159/AR.17.018

Investigation of coaxial laser cladding process parameters influence onto single pass clad geometry of tool steel

S. Locs[1,2], I. Boiko[1,*], P. Drozdovs[2], J. Dovoreckis[2] and O. Devoyno[3]

[1]Riga Technical University, Faculty of Mechanical Engineering, Transport and Aeronautics, Institute of Mechanical Engineering, Viskalu street 36A, LV-1006 Riga, Latvia
[2]Daugavpils University, Faculty of Natural Sciences and Mathematics, Parades street 1, LV-5401 Daugavpils, Latvia
[3]Belarusian National Technical University, Faculty of Mechanical Engineering B.Khmelnitsky street 9-6, BY220013 Minsk, Belarus
[*]Correspondence: irina.boiko@rtu.lv

Abstract. This paper is devoted to the investigation of the influence of technological parameters on the single pass clad geometry and quality as well as elemental composition in the clad after coaxial laser cladding (CLC). The objects of the investigation are components of expensive machines and tools for presswork needed to be repaired, i.e. refurbished for the future application with the goal of effective using of material resources in production. Nowadays such repair of worn tools is an actual task due to tendency for thrifty management of resources at affordable cost. Experimental work was carried out using CLC system, which consists of industrial robot and a ytterbium fiber laser with a core diameter of 100 μm, integrated to the coaxial powder supplying cladding head. During research separate cladding tracks of metal powder AISI M2 (particle size 53–150 μm) were deposited on the top surface of steel plates, which were grinded before treatment. This work's highlighted parameters for variation were laser scanning speed and laser beam focus plane distance. The clad geometry was examined on cross-sections with SEM. Elemental composition was determined by the X-ray spectroscopy analysis. Gladding beads with good surface quality were achieved. Cross-sectional observation presented that clads has a good fusion with the base material without exfoliation. Keyhole shape of molten substrate area was achieved, which leads to increase of the dilution value. The future research is needed to achieve stable quality of cladding, which is extremely necessary for industry.

Key words: coaxial laser cladding, toll steel, clad geometry, keyhole in penetration.

INTRODUCTION

Manufacturing process of any products involves use of natural resources. At the end of the life cycle of any product (Jolliet et al., 2003) its disposal, recycling or recovery is required. That is why the use of advanced technologies is of a great importance not only for industrial expansion but also reduces the factors of negative impact on the environment.

Laser cladding (LC) is an effective (advanced process) method for surface engineering, which allows to improve surface properties, like hardness, wear and

corrosion resistance, fatigue and strength. Due to a number of advantages, this process is successfully used for refurbishment and repair of high value parts and tools like engine components, turbines, dies, punches, press molds etc. (Toyserkani et al., 2005; Majumdar & Manna, 2013).

The major technological advantages of laser cladding are (Schneider, 1998):

- Possibility of precision energy supply;
- Low heat input, resulting in a small heat affected zone;
- Treatment is a non-contact process. There is neither tool wear nor mechanical forces impact on the workpiece;
- High accuracy and local surface treatment;
- Strong metallurgical bonding and very dense coatings;
- Slight heat deformation of the cladded component;
- Minimal dilution with the base material;
- High heating and cooling rates, resulting in a fine microstructure (metastable phases).

Another important application of LC is in additive manufacturing (AM) which appears in industry quite recently and is developing very rapidly. As it is known there are many names of this technology, for example: 'Laser Engineered Net Shaping' (LENS), 'laser powder fusion' (LPF), 'direct metal deposition' (DMD) etc. The main principle here is fabricating of single part layer by layer with a complex 3D shape by melting of injected metal powder under laser irradiation (Toyserkani et al., 2005). Combination of laser cladding technique with computer-aided design (CAD) and computer-aided manufacturing (CAM) processes creates a powerful tool for manufacturers in many engineering industries. As a result, this makes designing more flexible due to free-form modeling and quick change of design components. Manufacturing process does not require any intricate molds or dies. Advantages of this technology in comparison to traditional casting and machining allow to produce finished or semi-finished parts with complicated shape with high accuracy, economy of time and energy as well as material consumption, due to the fact that components are built by rather adding than removing material (in case of machining processes) (Xue, 2010; Majumdar & Manna, 2013). There are many parameters which have influence on this process. The main of them are laser power, laser scanning speed, powder mass feed rate and laser beam focus plane distance as well, as laser beam characteristics, continuous or pulsed wave light emission and also physical effects of the process (thermal distribution, fluid flow, phase transformation etc.). Variety of combinations of these parameters may have different effect on the clad geometry, functional properties and overall quality of the coating. By this reason experimental studies are still necessary for research of LC process (Oliveira et al., 2005).

This experiment was focused on investigation of single cladding bead formation with multiple cladding speed and laser beam focus disposition relatively the treatable surface. The purpose of the work is to determine the importance of highlighted parameters by performing statistical analysis and producing empirical models to achieve a single pass clad bead of high quality. This data is needed in order to determine appropriate regime of the process for the following experiments for surface cladding.

MATERIALS AND METHODS

The filler material used for LC was tool steel powder AISI M2 of spherical shape with particle size 53–150 μm. For substrates wear resistant high carbon steel (spring steel) DIN 66Mn4 plates were used with dimensions of 100 x 100 x 10 mm and the work surfaces mechanically grinded before treatment. Chemical compositions of the materials are listed in the next (Table 1).

Table 1. Chemical composition of powder AISI M2 (1) and substrate DIN 66Mn4 (2)

	Element content, wt%						
	C	Mn	Si	Mo	Cr	V	W
1	0.85–1.05	0.20–0.40	0.20–0.40	4.50–5.50	3.75–4.50	1.60–2.20	5.50–6.80
2	0.62–0.70	0.90–1.20	0.17–0.37	–	< 0.25	–	–

Experimental work was carried out using the precise LC equipment, which consists of industrial 6 axis robot KR30HA and 2 axis DKP-400 positioner (Kuka) and ytterbium single mode fiber laser with a core diameter of 100 μm YLR-1000 (IPG Laser) which ensures Gaussian beam intensity profile and emits on wavelength 1,070 nm. Laser with variable output power up to 1,000 W and was integrated to the coaxial powder supplying cladding head with the optical system WT03 (Permanova Lasersystem). Powder mass feeding was performed with powder feeder TWIN-10-C (Sulzer Metco), where the argon was used as a carrier gas and as a shielding gas as well in order to prevent oxidation of the powder and a molten pool. The heating temperature was measured after each deposited track using high-temperature infrared thermographic camera InfRec R300 (Nippon Avionics). Substrate temperature after single run didn't exceed 100 °C. The laser cladding equipment and experimental performance are in the next (Fig. 1).

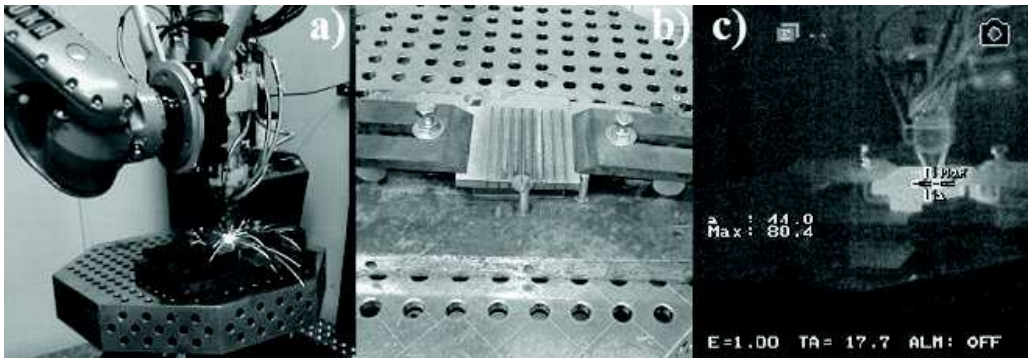

Figure 1. Laser cladding: general view of equipment (a); experimental sample with generated clad tracks (b); infrared camera shot after deposition of single track (c).

As the first step of the experiment preliminary setting-up was performed, where the numbers of single tracks was deposited at various regimes to achieve continuous and uniform clad beads in order to determine the range of process parameters for the following design of experiment (DOE). Then, with aim to investigate the process responses, single clad tacks were produced by experimental plan, which consisted of multiple combination of laser scanning speed and value of laser beam defocus. In order

to examine full interaction of chosen factors experimental work was carried out against planned four level Taguchi's Orthogonal Array L_{16} for two defocusing directions i.e. (f_1: from -3 to 0) and (f_2: from +3 to 0) with step of 1 mm. Therefore 28 single tracks were produced in total. Experimental factors and levels according to defocusing directions are presented in the next (Tables 2, 3). The other parameters for every cladded track have been fixed and they were as following: laser power was set on maximum value 1,000 W; carrier gas flow (Ar) 5 l min^{-1}; shielding gas flow (Ar) 15 l min^{-1}; powder feed rate 7 g min^{-1}, laser beam focal distance 200 mm.

Table 2. Factors and levels for negative direction of defocus

Factors	Levels			
Cladding speed, m s^{-1}	0.025	0.020	0.015	0.010
Focus disposition, mm	-3	-2	-1	0

Table 3. Factors and levels for positive direction of defocus

Factors	Levels			
Cladding speed, m s^{-1}	0.025	0.020	0.015	0.010
Focus disposition, mm	+3	+2	+1	0

Plates with experimental clad beads were transversely cross-sectioned, then polished and etched with Nital (4%). Each produced clad bead was examined using scanning electron microscope TESCAN-VEGA-LMU II (SEM). Quality characteristics of LC beads were evaluated by measuring clad bead cross-section geometry, content of pores and measuring of elemental composition of alloy elements (AE). Geometry features were determined by studying of the SEM micrographs using 'Measurement' module of software 'VegaTC'. Schematic view and geometrical characteristics of the single clad bead in cross section are represented in the next (Fig. 2). Elemental composition was determined by energy dispersive X-ray spectroscopy analysis (EDS module INCAx-act Oxford Instruments, attached to SEM). The used matrix of experimental design with measures are presented in the next (Table 4).

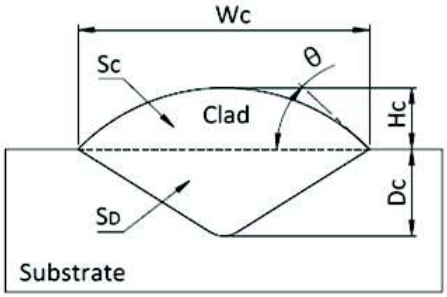

Figure 2. Schematic view and geometrical characteristics of clad bead.

Table 4. Parameters and cross-sectional measurements of clad beads

No	F mm	V m s^{-1}	H mm	W mm	D mm	Θ °	S_D mm^2	S_C mm^2	S_P mm^2	Pores %	ΣAE wt%
1	-3	0.025	0.21	1.50	1.44	39	1.12	0.23	0.00	0	2.51
2	-3	0.020	0.28	1.71	1.57	30	0.99	0.19	0.03	3	3.60
3	-3	0.015	0.37	1.90	1.67	34	1.32	0.31	0.05	3	3.39
4	-3	0.01	0.45	2.13	1.81	43	1.66	0.45	0.09	4	2.93
5	-2	0.025	0.29	1.44	1.64	45	1.32	0.48	0.08	4	2.51
6	-2	0.020	0.42	1.77	1.60	43	1.85	0.53	0.12	5	5.60
7	-2	0.015	0.44	1.95	1.96	55	2.37	1.05	0.11	3	4.01
8	-2	0.01	0.69	2.29	2.02	47	2.24	0.64	0.02	1	5.62
9	-1	0.025	0.38	1.14	2.16	64	1.23	0.33	0.00	0	3.51
10	-1	0.020	0.39	1.39	2.33	67	1.34	0.35	0.01	0	3.53
11	-1	0.015	0.49	1.75	2.23	65	1.68	0.59	0.00	0	4.85
12	-1	0.010	0.74	2.17	2.37	57	2.39	0.94	0.00	0	6.19
13	0	0.025	0.36	1.17	2.23	53	1.11	0.25	0.00	0	3.35
14	0	0.020	0.37	1.45	2.33	57	1.33	0.45	0.00	0	4.76
15	0	0.015	0.48	1.68	2.51	63	1.72	0.51	0.00	0	3.62
16	0	0.010	0.70	1.97	2.41	62	2.22	0.95	0.01	0	5.49
17	3	0.025	0.13	1.42	1.08	17	0.72	0.10	0.00	0	3.01
18	3	0.020	0.15	1.55	1.05	23	0.89	0.13	0.00	0	2.20
19	3	0.015	0.21	1.85	1.14	22	1.15	0.24	0.00	0	3.31
20	3	0.010	0.34	2.15	1.31	32	1.67	0.48	0.00	0	4.59
21	2	0.025	0.17	1.51	1.40	24	1.02	0.16	0.08	7	2.18
22	2	0.020	0.21	1.64	1.54	27	1.22	0.19	0.06	4	2.14
23	2	0.015	0.23	1.83	1.58	27	1.47	0.29	0.06	4	3.13
24	2	0.010	0.38	2.19	1.58	32	1.95	0.56	0.01	1	3.73
25	1	0.025	0.25	1.57	1.51	29	0.97	0.26	0.11	9	3.21
26	1	0.020	0.30	1.65	1.65	37	1.18	0.33	0.10	7	4.94
27	1	0.015	0.40	1.88	1.96	49	1.56	0.51	0.00	0	4.33
28	1	0.010	0.53	2.07	2.31	55	2.19	0.72	0.04	2	4.41

RESULTS AND DISCUSSION

Morphology

During laser scanning melt pool is generated by melting of base material together with injected powder particles, which forms after solidification a congeneric clad bead. By visual observation of clads surfaces it was noticed that all of them have a good fusion with the base material – no surface defects as pores, crack or exfoliation were found. Surface topology of a part of produced clad bead in dependence of parameters combination is presented in the next (Fig. 3).

Geometrical characteristics of each single track in cross-section were determined by measures of clad height (H_C), width (W_C), contact angle (θ), depth of penetration (D_C), clad area (S_C), penetration area (S_D) and total pores area (S_P). These measured characteristics are shown below (Fig. 4, a and b).

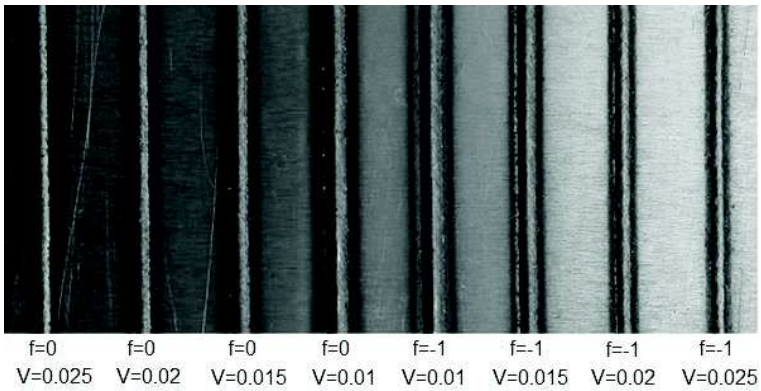

Figure 3. Surface topology of single clad beads, where f – focus deposition, mm; V – cladding speed, m s^{-1}.

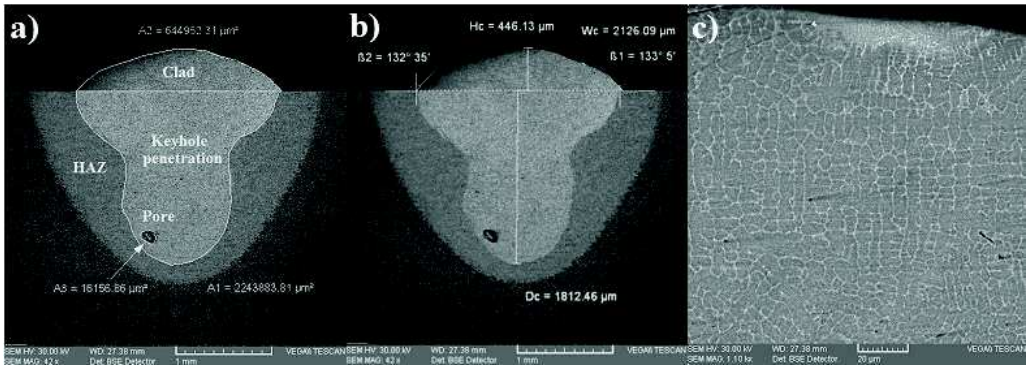

Figure 4. Clad cross sections SEM images of No.4 clad bead with geometrical measures and higher magnification micrograph of clad top region.

As it can be seen, the clearly distinguishable zones of the clad bead in comparison with the base material can be defined. The microstructure of clad beads (Fig. 4, c) had a mixture of cellular and dendritic solidification grain structures. In the upper and midle zones of clad grains were mostly cellular, however in the area bondering to the inerface with base material basicaly dendritic. Due to processing by a highly concentrated energy source clad area apparently has martensite-austenite microstructure with carbide eutectic at grain boundaries ($CrWMo_nC_m$) as it was mentioned in (Grigor'yanc et al., 2012). Typical martensitic needles inside grains weren't observed, presumably structureless martensite (hardenite) takes place, which is often a mixture of martensite and austenite without acicular structure, and usually is detected when heating by a concentrated energy flow (Kirillov et al., 1996; Isakin et al., 2015). Heat affected zone (HAZ) in the peripheral area of clad bead can also be observed. All produced clads have significant penetration inside of substrate, which have keyhole geometry as a result of high laser beam intensity. Application of such a deep penetration in the laser cladding process is assumed for creation of first layer onto tool steel substrate with aim to achieve smooth gradient of mechanical properties of the coating-substrate system to provide better resistance to external stress during tool operation in the press working process. It was

also noticed, that a part of clad beads contain pores, what also might be the reason of high energy input, because the melt of irradiated materials passes to vapor state, and this leads to appearance of gas bubbles, which in their turn due to a rapid solidification of the melt pool stay entrapped in the clad bead (Majumdar & Manna, 2013; Gong et al., 2014). The generalized list of compared SEM micrographs of clad beads profiles according to varied process parameters is represented in the next (Fig. 5).

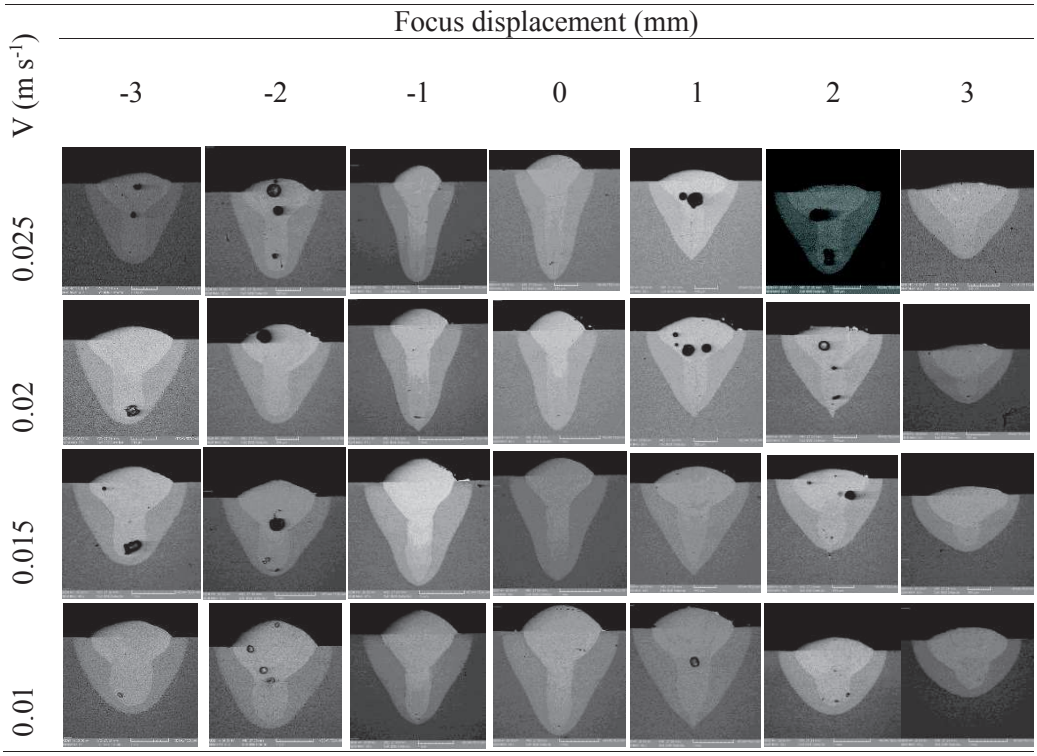

Figure 5. SEM micrographs array of clad beads under combination of parameters, where V – cladding speed.

Data analysis

Clad beads quality was evaluated using the following features: geometrical characteristics (clad height, width, depth of penetration and contact angle), porosity percentage and content of alloying elements in the clad zone. In order to determine influences of the process parameters onto chosen responses predictive equations were build using regression analysis. The first order regression model was used with the following polynomial expression:

$$y = \beta_0 + \sum_{i=1}^{k} \beta_i x_i + \varepsilon. \quad (1)$$

For evaluating of statistical significance created models were also tested by analysis of variance (ANOVA).

Clad height and width characterize productivity of LC process, by this reason it is important to achieve maximum values of these parameters. As it can be seen from the next (Fig. 6) clad height and width increase with decrease of cladding velocity. Relatively to laser beam defocus very similar nature of distributions for both of these parameters can be observed. The highest values of a clad height can be achieved by defocusing laser beam at 0 to -2 mm, where maximal values were 0.4–0.7 mm according to change of velocity regimes, e.g. smallest value for highest cladding speed. Meanwhile clad width had the worst results of focus disposition at 0 to -1 mm, but the largest values mainly correspond to defocusing at -2 mm with amount of 1.4–2.3 mm, where smallest value for highest cladding speed respectively. Optimal combination of both of these geometrical features characterizes ratio of clad height to width (wh), the highest value of this index was 1.6 mm and it corresponds to the lowest speed (0.01 m s^{-1}) and to defocus at -2 and -1 mm.

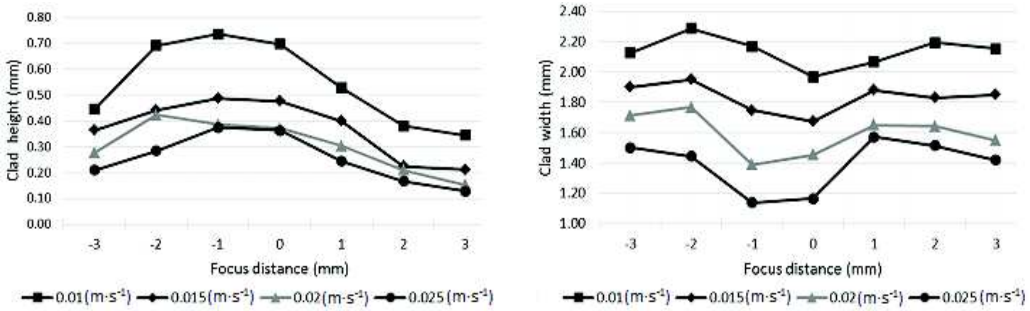

Figure 6. The effect of focus displacement onto the clad height (a) and the clad width (b).

Clad beads depth of penetration should be as minimal as possible, because it identifies the dilution ratio, which in its turn presents rate of intermixing of clad layer and base material (Schneider, 1998). Contact angle (wetting angle) is also important parameter that indicates the quality of the clad. This angle defines statement of surface wettability and has to be smaller than 90°. In order to ensure good adhesion the optimal value of contact angle should be as $\cos(\theta) \rightarrow 1$ (Toyserkani et al., 2005). As it is seen in the Figure below (Fig. 7) both of these parameters represent very similar relationship to the velocity distributions towards to the defocus. Minimal depth of penetration corresponds to the highest velocity and the largest focusing distance (+3 mm) – that is below the treatable surface. The smallest values of clad bead depth were 1.1–1.3 mm, where the smallest one was for the highest cladding speed. Contact angle represents analogue dependency – the smallest angle corresponds to the highest velocity and the largest focusing distance. The smallest values this parameter showed by focusing laser beam at +3 mm and these values varied from 17° to 32°. The overall contact angle of produced clads was varying in range from 17° to 67°, that satisfies surface wettability conditions.

Analysis of the clad beads quality was also carried out on the basis of alloy elements content and porosity percentage in the clad. During LC process due to melting of filler and base material, oxidation and intermixing of melt and base occurs, which leads to exhaustion of the alloying components concentration in the clad layer, thereby mechanical properties become worse. The content of alloy elements was examined for each clad layer using the EDS analysis.

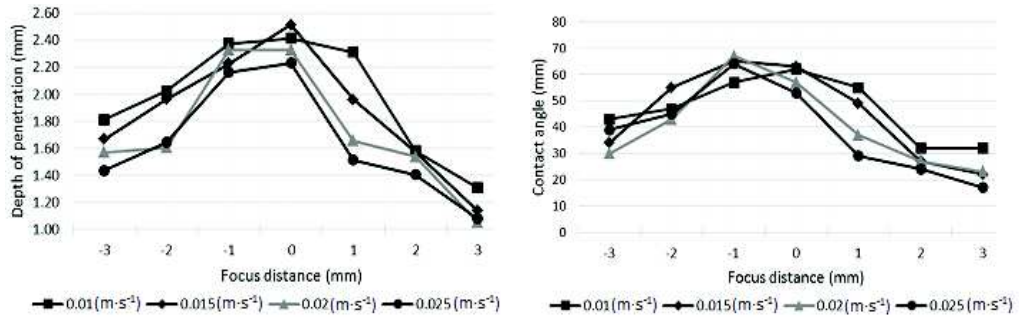

a) b)

Figure 7. The effect of focus displacement onto the clad depth (a) and the clad contact angle (b).

In order to investigate interrelation, as a response parameter was determined by a total amount of mass fraction for the carbide-forming elements such as Cr, W, Mo, V. As it can be seen from the next picture (Fig. 8, a) maximal values correspond to the defocus from -2 to 0 with pick on -1 mm. It was noticed that by increasing of cladding speed exhaustion of the alloying components concentration increases. The reason most likely is the following: due to shielding effect produced by vapors generated during the melting of powder particles in the zone exposed by laser radiation (Devoyno et al., 2012).

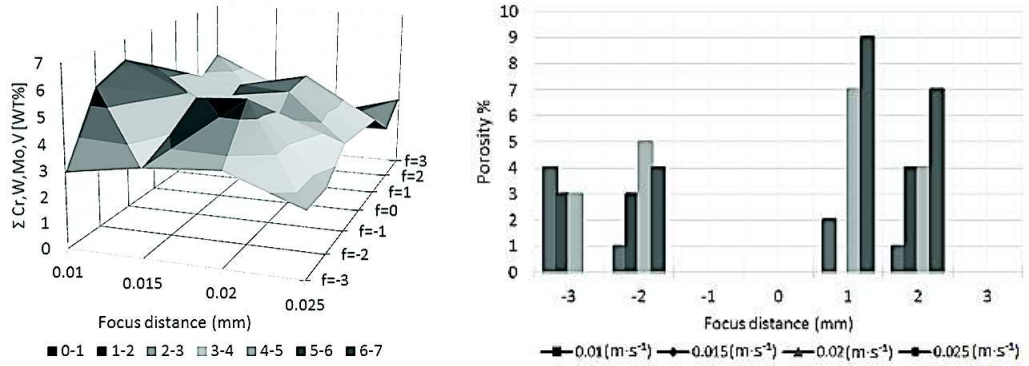

a) b)

Figure 8. The effect of focus displacement onto the EA content (wt%) (a) and the porosity percentage (b).

Analysis of porosity showed irregular distribution order of values. The degree of porosity was determined by analysis of SEM micrographs and was expressed as the areas ratio of the total pores surface area towards the clad bead overall surface area. It has to

be pointed that the amount of common pores increases with the increase of cladding speed. The reason is that due to material evaporation when cladding at higher speed gas bubbles don't have time for rising to the surface. As it can be seen from the next (Fig. 8, b) the largest value reached up to 9%, but relatively to all studied clad beads average index was 2%. Meanwhile, when processing with laser beam defocus at such values as -1; 0 and 3 mm, clad beads were free of pores.

The significance of correlations between the independent variables (focus distance and cladding speed) and dependent variables (clad height, width, depth, contact angle, porosity and AE content) were evaluated by using ANOVA. Analysis carried out by separate plans according to opposite directions of laser beam defocusing i.e. negative (-f) and positive (+f) defocus directions (ND and PD) away from the focal plane. ANOVA was performed with a confidence level of 95% (*P*-value of 0.05). Additionally, empirical models were generated by means of regression analysis based on the measured responses.

Table 5. ANOVA for the clad height: *DF* – degree of freedom, *SS* – sum of squares, *MS* – mean squares

	Negative defocus				
Source	*DF*	*SS*	*MS*	*F*	*P*
Model	2	0.282	0.141	28.1	< 0.0001
-f	1	0.049	0.049	9.67	0.0080
V	1	0.234	0.234	46.53	< 0.0001
Residual	13	0.065	0.005		
Total	15	0.347			
Positive defocus					
Model	2	0.317	0.158	60.48	< 0.0001
+f	1	0.172	0.172	65.47	< 0.0001
V	1	0.145	0.145	55.49	< 0.0001
Residual	13	0.034	0.003		
Total	15	0.351			

Table 5 represents ANOVA for the clad height. *F*-values 28.1 and 60.48 indicate that the models are statistically significant, particularly high value is for *PD* plan. *P*-values of less than 0.05 indicate that focal distance (f) and velocity (V) are significant model terms. Concerning *PD* plan terms are nearly equivalent, meanwhile for *ND* plan cladding speed has much greater effect. Regression analysis gives the predictive equations for *ND* plan (2) and for PD plan (3) respectively. Coefficient of determination (R^2) for *ND* equals to 0.81 and R^2 for *PD* equals to 0.9 and proves high convergence between experimental and predicted results. Empirical model for *ND* plan (2) demonstrates that clad height increases by increasing of focal length and decreasing of cladding speed. The model for *PD* plan (3) indicates clad height increase by decreasing both of these factors.

$$H_{C(-f)} = 0.892 + 0.0493\,f - 21.6\,V, \quad (2)$$

$$H_{C(+f)} = 0.763 - 0.0926\,f - 17.1\,V. \quad (3)$$

Table 6 shows ANOVA for clad width, which represents extremely high models significance: *F*-value for *ND* plan was 87.96 and for the *PD* plan model *F*-value was 51.4. As it is seen from both model terms *F*-values, cladding speed has considerably the largest effect on clad width.

Table 6. ANOVA for the clad width

	Negative defocus				
Source	*DF*	*SS*	*MS*	*F*	*P*
Model	2	1.669	0.834	87.96	< 0.0001
-f	1	0.194	0.194	20.47	0.0010
V	1	1.474	1.474	155.44	< 0.0001
Residual	13	0.123	0.009		
Total	15	1.792			
Positive defocus					
Model	2	1.087	0.543	51.4	< 0.0001
+f	1	0.057	0.057	5.42	0.0370
V	1	1.029	1.029	97.38	< 0.0001
Residual	13	0.137	0.011		
Total	15	1.224			

As it can be seen from predictive equation (4), which correspond to *ND* plan, clad width increases by decreasing both of model terms. In the case of *PD* plans equation (5), clad width increases by increasing of focal length and by decreasing of cladding speed. R^2 had also high values: for *ND* it equals to 0.93 and for *PD* – to 0.89.

$$W_{C(-f)} = 2.52 - 0.0985\, f - 54.3\, V, \tag{4}$$

$$W_{C(+f)} = 2.44 + 0.0535\, f - 45.4\, V. \tag{5}$$

Analysis data concerning the clad depth is shown in the next Table 7. ANOVA represents also very high significance of the models: *F*-value for *ND* plan was 61.46 and for the *PD* plan *F*-value was 102.72. In this case the main effect showed focus distance, this was considerably higher than the cladding speed.

Table 7. ANOVA for the clad depth

	Negative defocus				
Source	*DF*	*SS*	*MS*	*F*	*P*
Model	2	1.672	0.836	61.46	< 0.0001
-f	1	1.474	1.474	108.37	< 0.0001
V	1	0.198	0.198	14.55	0.0020
Residual	13	0.177	0.014		
Total	15	1.849			
Positive defocus					
Model	2	3.508	1.754	102.72	< 0.0001
+f	1	3.22	3.22	188.84	< 0.0001
V	1	0.284	0.284	16.60	0.0010
Residual	13	0.222	0.017		
Total	15	3.730			

The below given equation (6) for *ND* plan represents that the clad depth decreases by decreasing of the focus distance and by increasing of cladding speed. In the case of *PD* plan (7) clad depth decreases by increasing of both of model terms. R^2 for these models showed very high values: for *ND* it equals to 0.90 and for *PD* – to 0.94.

$$D_{C(-f)} = 2.77 + 0.272 f - 19.9 V, \quad (6)$$

$$D_{C(+f)} = 2.74 - 0.402 f - 23.8 V. \quad (7)$$

The next one analysis carried out for the clad contact angle showed in the next Table 8 represents that more significant model was for *PD* plan. Generally *F*-value for ND plan was 14.02 and for the *PD* plan *F*-value was 64.69. The focus distance is again appearing as a dominant factor. Velocity in case of *ND* plan revealed insignificance of model term.

Table 8. ANOVA for the clad contact angle

	Negative defocus				
Source	*DF*	*SS*	*MS*	*F*	*P*
Model	2	1,385.45	692.72	14.02	0.0010
-f	1	1,361.25	1,361.25	27.54	0.0002
V	1	24.2	24.2	0.49	0.5000
Residual	13	642.55	49.43		
Total	15	2,028.0			
Positive defocus					
Model	2	3,372.1	1,686.1	64.69	< 0.0001
+f	1	2,916.11	2,916.11	111.89	< 0.0001
V	1	456.01	456.01	17.50	0.0010
Residual	13	338.81	26.06		
Total	15	3,710.94			

Predictive equation for the *ND* plan (8) showed that contact angle decreases by decreasing of focus distance and by increasing of cladding speed. In the case of *PD* plan (9) this response decreases by increasing of both of model terms. R^2 for these models was as following: for *ND* plan it equals to 0.68 and for *PD* plan – to 0.91.

$$\theta_{(-f)} = 67.7 + 8.25 f - 220 V, \quad (8)$$

$$\theta_{(+f)} = 72.9 - 12.1 f - 955 V. \quad (9)$$

In order to analyze process parameters influence on to porosity ANOVA was performed in the same way as for studying of geometry characteristics. As it can be seen in the next Table 9 model significance can be seen just in case of *ND* plan, where *F*-value was 5.22, but for *PD* plan *F*-value was 1.47, which showed insignificance of model to this response. However in case of *ND* plan the analysis defined that only defocus had an effect on degree of porosity.

Table 9. ANOVA for the porosity

	Negative defocus				
Source	*DF*	*SS*	*MS*	*F*	*P*
Model	2	23.125	11.563	5.22	0.022
-f	1	23.113	23.113	10.43	0.007
V	1	0.0125	0.0125	0.006	0.941
Residual	13	28.813	2.216		
Total	15	51.938			
Positive defocus					
Model	2	26.500	13.250	1.47	0.266
+f	1	0.05	0.05	0.005	0.942
V	1	26.45	26.45	2.93	0.11
Residual	13	117.25	9.019		
Total	15	143.75			

As it is seen from the predictive equations (10) and (11) that pores content decrease by increasing of focus distance in case for both of defocusing plan. R^2 was equal to 0.45 in case of *ND* plan and for *PD* plan equal to 0.18, and it represents too weak conformity of the calculated and measured values.

$$P_{(-f)} = - 0.09 - 1.07 f - 5.0 V. \quad (10)$$

$$P_{(+f)} = - 1.83 - 0.05 f + 230 V. \quad (11)$$

ANOVA analysis of the effects of parameters on the total amount of alloy elements (Cr, W, Mo, V) is presented in the next Table 10. The models *F*-values of 5.68 for *ND* plan and 8.45 indicated significant statistical relationships. It was found out that in case of *PD* plan both the model terms were significant. The analysis indicated only insignificance of defocus for *ND* plan.

Table 10. ANOVA for the content of AE

	Negative defocus				
Source	*DF*	*SS*	*MS*	*F*	*P*
Model	2	9.567	4.783	5.68	0.017
-f	1	2.705	2.705	3.21	0.096
V	1	6.862	6.862	8.15	0.014
Residual	13	10.944	0.842		
Total	15	20.511			
Positive defocus					
Model	2	8.949	4.474	8.45	0.004
+f	1	4.068	4.068	7.68	0.016
V	1	4.88	4.88	9.21	0.010
Residual	13	6.89	0.530		
Total	15	15.835			

Predictive equations demonstrate EA content increase by focusing laser beam towards the focal plane. Velocity has a negative effect; thereby its increase leads to minimization of EA in the clad. R^2 had very close values, which for *ND* plan were equal to 0.47, in case of *PD* plan – to 0.56 and by converting these values to the correlation

coefficients (R) 0.69 and 0.75 respectively; so they present appreciable relationship between the experimental and predicted results. Therefore, for the further research the optimal regime can be determined by relying onto created model:

$$EA_{(-f)} = 6.69 + 0.368\,f - 117\,V, \quad (12)$$

$$EA_{(+f)} = 6.06 - 0.451\,f - 98.8\,V. \quad (13)$$

CONCLUSIONS

The quality of laser cladding coating first of all depends on ability to create a single clad with the necessary characteristics. The tool steel clad beads were deposited using different combinations of process parameters including laser beam focus displacement and cladding speed. The produced clads have been evaluated by geometrical parameters, content of alloying components, degree of porosity and the results have been statistically analyzed. The examination of the obtained results shows the following:

- Solid clad with good fusion bond and fine microstructure has been achieved in this research, but porosity is still a problem; presumably due to a high power intensity and keyhole behavior effect.
- It was assumed that by creation of the first layer of laser cladded coatings with keyhole in penetration could ensure smooth gradient of mechanical properties of the coating-substrate system to provide better resistance to external stress during tool operation in the press working process.
- The maximal value of combination of clad height and width (wh) was achieved at the lowest cladding speed (0.01 m s^{-1}) and by defocusing laser beam at -2 to -1 mm.
- The minimal depth of penetration corresponds to the highest cladding speed and the largest focusing distance (+3 mm) – when the focus plane was displaced below the treatable surface.
- The contact angle of the produced clads was varying in range from 17° to 67°, the smallest values correspond for +3 mm defocus and by the highest velocity.
- The maximal content of alloy elements (Cr, W, Mo, V) was discovered by defocus at -1 mm and by the lowest cladding speed (0.01 m s^{-1}).
- Porosity had irregular distribution order, but nevertheless the largest average value corresponds to the highest cladding speed. The largest value of 9% was detected by defocus at +1 mm, but relatively to all the studied clad beads the average index was 2%. Meanwhile by processing with laser beam defocus at -1; 0 and +3 mm, clad beads were free of pores.
- ANOVA showed significant relationships between the process parameters and characteristics of clad beads geometry for both defocus directions with the exception of cladding speed and contact angle correlation in case of negative defocus.
- Statistical analysis of porosity showed that only focus displacement in negative direction correlates with measured data.
- The analysis of alloy elements content indicated significant relationships of all of model terms except of defocus in negative direction.

– The developed empirical models are found to be able to predict the geometry of clad beads and alloy element content in it within a confidence level more than 95%. In the following research the optimal regime can be determined by relying onto created models. To determine nature of the pore-formation the extended studies are required.

ACKNOWLEDGEMENTS. The authors gratefully acknowledge financial support from the company 'Magistr Ltd' (Daugavpils, Latvia).

REFERENCES

Devoyno, O.G., Drozdov, P.S., Dovoretskiy, Y.B., Kardapolova, M.A., Lutsko, N.I. & Tamanis, E. 2012. Influence of laser cladding parameters on the distribution of elements in the beads of nickel-based Ni–Cr–B–Si alloy. *Latvian journal of physics and technical sciences* **4**, 61–70.

Gong, H., Gu, H., Zeng, K., Dilip, J.J.S., Pal, D. & Stucker, B. 2014. Melt Pool Characterization for Selective Laser Melting of Ti-6Al-4V Pre-alloyed Powder. In*: 25th Annual International Solid Freeform Fabrication Symposium*. The University of Texas, Austin, USA, pp. 256–267.

Jolliet, O. Margni, M., Charles, R., Humbert, S., Payet, J., Rebitzer, G. & Rosenbaum, R. 2003. IMPACT 2002+: A New Life Cycle Impact Assessment Methodology. *International journal of life cycle assessment* **8**(6), 324–330.

Majumdar, J. & Manna, I. 2013. *Laser-Assisted Fabrication of Materials*. Springer, Berlin, 485 pp.

Grigor'yanc A.G., Misyurov, A.I., Tretyakov, P.S. & Staverty, A.Y. 2012. Investigation of influence of laser radiation type on the structure and properties of tool steel with cladded coatings. *Science and education: Scientific Periodical of The Bauman* **FS77**(48211), 11–20. (in Russian)

Isakin I.A. & Zykov, I.Y. 2015. Structure and properties of coatings based on steel 10R6M5 after surface laser melting. In: *Materials processing: modern problems and solutions: a collection of works of the All-Russian Scientific and Practical Conference of Young Scientists, Postgraduates and Students*. TPU, Tomsk, Russian Federation, pp. 123–126. (in Russian)

Kirillov N.B., Krivoshchyokov, V.L. & Shlyonov, Y.V. 1996. On some questions of the strength of the surface during high-speed heat treatment. *Belgorod State University Scientific bulletin* **2***,* 3–9. (in Russian)

de Oliveira, U. Ocelik, V. & De Hosson, J.Th.M. 2005. Analysis of coaxial laser cladding process conditions. *Surface coatings&Technology* **197**(2–3), 127–136.

Schneider, M.F. 1998. *Laser cladding wth powder*. Twente (Netherlands), University, Dissetation, Enschede, 177 pp.

Toyserkani, E., Khajepour, A. & Corbin, S. 2005. *Laser Cladding*. CRC Press LLC, New York, 263 pp.

Xue, L. 2010. Laser consolidation: a rapid manufacturing process for making net-shape functional components. In Lawrence, J., Pou, J., Low, D.K.Y. & Toyserkani, E. (eds): *Advances in laser materials processing.* Woodhead Publishing Limited, UK, pp. 492–534.